Superfluid properties of ultracold fermionic atoms in two-dimensional optical lattices

Yusuke Fujihara,[1] Akihisa Koga,[2] and Norio Kawakami[1]
[1]*Department of Physics, Kyoto University, Kyoto 606-8502, Japan*
[2]*Department of Physics, Tokyo Institute of Technology, Tokyo 152-8551, Japan*
(Received 3 January 2010; published 23 June 2010)

We investigate two-component ultracold fermionic atoms with attractive interactions trapped in a two-dimensional optical lattice at zero temperature. By introducing a superfluid trial state with spatially modulated order parameters, we perform the variational Monte Carlo simulations to treat the correlation effects beyond mean-field treatments. It is shown that there appears a strong tendency to the formation of a density wave state in the regions with specific values of local atom density. We then analyze two kinds of perturbations to the superfluid state and show that a coexisting state of superfluid and density wave ordering, a sort of supersolid state, can be stabilized. It is discussed how the trap potential and the resulting spatial modulation of the superfluid state affect the momentum distributions and the noise correlation functions.

DOI: 10.1103/PhysRevA.81.063627 PACS number(s): 03.75.Ss, 05.30.Fk, 71.10.Fd

I. INTRODUCTION

Optical lattice systems, where ultracold atoms are loaded in a periodic potential, have attracted much interest since the successful observation of the superfluid-Mott insulator transition in bosonic atoms [1–3]. One of the great advantages for these systems is high controllability of quantum parameters such as the interactions between atoms, the lattice geometry, etc., which can be easily manipulated by tuning a magnetic field and the intensity of the lasers. In addition, the optical lattices provide superclean systems in the sense that they do not suffer from lattice defects and impurities, in contrast to solid-state materials, hence providing an ideal stage for studying intriguing quantum phases of condensed matter [4–7].

Superfluidity of fermionic atoms is one of the most fascinating phenomena in this context. Recent experiments make it possible to realize the superfluid state in an optical lattice [8], which should certainly stimulate further systematic studies of unconventional superfluidity in the near future. Extensive theoretical investigations on the superfluid state of fermions in an optical lattice have treated a wide variety of remarkable phenomena, such as the BEC-BCS crossover [9–11], the superfluid-Mott insulator transition [12–16], the Fulde-Ferrell-Larkin-Ovchinnikov-type superfluid state [17–23], and the high-temperature superfluid state in (quasi-) two-dimensional (2D) lattices [24,25].

In such optical lattice systems, it is important to consider the effect of a trap potential, which is inherent in the experiments in cold atoms. In contrast to bulk systems, the density profile thus reflects the shape of the confining potential, and therefore the superfluid state with a nonuniform density profile should be realized. Though the situation makes the theoretical treatments more complicated, it provides an opportunity to explore some novel quantum phenomena. Among others, recent theoretical studies [26–30] have suggested that a supersolid state, where a density wave state coexists with a superfluid state, may be stabilized in fermionic systems due to the trap potential. Since most of those numerical investigations of the supersolid state are based on local approximations, it is desirable to explore to what extent intersite correlations are relevant in realizing the supersolid state in optical lattice systems.

In this article, we study the ground-state properties of fermions with attractive interactions in a 2D optical lattice with particular emphasis on the correlation effects on superfluidity. As mentioned earlier, it is important to take into account the effects of inhomogeneity due to the trap potential. To this end, we first examine a mean-field state with spatially modulated superfluid ordering by solving the Bogoliubov-de Gennes (BdG) equations self-consistently. This state is used to prepare a proper trial state which can incorporate the atom correlations in a trapped system. We then perform the variational Monte Carlo (VMC) calculation [31,32] to treat on-site and intersite atom correlations systematically. We also investigate how sensitive the system is to small perturbations which may stabilize the density wave state, from which we argue a possibility of the supersolid state. Finally we investigate two observable quantities which should reflect the nature of the spatially modulated superfluid state in the trap potential.

This article is organized as follows. We introduce the model Hamiltonian in Sec. II and perform the VMC calculation to take into account the correlation effects on superfluidity in Sec. III. The roles of on-site as well as intersite correlations are elucidated. We then analyze the instability toward a density wave state and argue a possibility of the supersolid state in Sec. IV. In Sec. V, as experimentally accessible quantities, we show the momentum distributions and the noise correlation functions for the superfluid state. A brief summary is given in the last section.

II. MODEL

We study the ground-state properties of ultracold fermionic atoms with attractive interactions in a 2D optical lattice. Here we consider a system of the mixture of two-component fermions with equivalent hopping matrices. Experimentally, the situation has been realized by using the fermionic isotopes of ytterbium (^{171}Yb and ^{173}Yb) [33] or two accessible hyperfine levels of ^{40}K with $|F,m_F\rangle = |9/2,-9/2\rangle,|9/2,-7/2\rangle$ [34], where F and m_F are the total atomic angular momentum and its magnetic quantum number, respectively. We specify the two different internal degrees of freedom by pseudospin

indices $\sigma = \uparrow, \downarrow$ and consider the following Hubbard model in order to describe the ultracold atoms in an optical lattice [35,36],

$$\mathcal{H} = -t \sum_{\langle i,j\rangle\sigma} (c^{\dagger}_{i\sigma} c_{j\sigma} + \text{H.c.}) + \sum_{i\sigma} (V_i - \mu) n_{i\sigma} - U \sum_i n_{i\uparrow} n_{i\downarrow}, \tag{1}$$

where $c^{\dagger}_{i\sigma}$ ($c_{i\sigma}$) is the creation (annihilation) operator of a fermion with spin σ at site i and $n_i = \sum_i n_{i\sigma} = \sum_{i\sigma} c^{\dagger}_{i\sigma} c_{i\sigma}$ is the number operator. t and U (>0) are the hopping matrix between the nearest-neighbor sites and the on-site attractive interaction, which are experimentally controllable by tuning the intensity of the laser and by making use of the Feshbach resonance techniques [37]. V_i is a harmonic trap potential imposed on the lattice, which causes inhomogeneous properties of the system.

In this study, we consider a 2D square lattice system with $L \times L$ sites and fix the total number of atoms as $N_\uparrow = N_\downarrow$, where $N_\sigma = \sum_i n_{i\sigma}$. The harmonic trap potential at site $i = (x,y)$ $(0 \leqslant x, y \leqslant L-1)$ is given as

$$V_{i=(x,y)} = \frac{2V_0}{L(L-2)} \left\{ \sum_{\xi=x,y} \left(\xi - \frac{L-1}{2} \right)^2 - \frac{1}{2} \right\}, \tag{2}$$

where $V_i = 0$ at four sites around the center of the system, $V_i = V_0$ at the corners and we use t as the energy unit. We properly set the system size L and the chemical potential μ so as to conserve the number of atoms under the condition that the atom density is almost zero at the edges of the system. Therefore, in our calculations, we do not find any unphysical properties which originate from the boundary condition. In the following, we investigate the superfluid properties of fermionic atoms at zero temperature. To take into account the correlation effects in the trap potential, we make use of the BdG equations and introduce a proper trial state for the VMC simulations.

III. PROPERTIES OF SUPERFLUID STATE

For fermionic atoms with attractive interactions, the isotropic Cooper pairs should be formed between atoms with opposite spins. Therefore, the ground state expected in our system is a spatially modulated superfluid state with an s-wave-like symmetry. A number of theoretical studies have already been done for the systems with considerable success. However, most of them are based on the mean-field approximations or the local density approximations (LDAs), and thus the correlation effects in trapped systems have not been considered sufficiently. Therefore, in this section, we perform the VMC calculation to take into account the correlations effects. In particular, this method is not based on the LDA, so that the spatially extended correlation effects in trapped systems can be easily treated. Here we introduce the following trial state to investigate the spatially modulated superfluid state:

$$|\Psi\rangle = \exp\left[\sum_i \alpha_i n_{i\uparrow} n_{i\downarrow} + \alpha' \sum_i \hat{Q}_i \right] |\Phi\{\Delta_i\}\rangle, \tag{3}$$

where, $|\Phi\{\Delta_i\}\rangle$ is a mean-field state with site-dependent pair potentials Δ_i, which is explicitly given in what follows. Here $\{\alpha_i\}$ are a set of the site-dependent Gutzwiller variational parameters [32], which take into account the on-site correlation effects. α' is the so-called spinon-spinon binding parameter [38] which can incorporate intersite correlations, where $\hat{Q}_i = \sum_\sigma \hat{s}_{i\sigma} \prod_\tau (1 - \hat{s}_{i+\tau\bar{\sigma}})$, $\hat{s}_{i\sigma} = n_{i\sigma}(1 - n_{i\bar{\sigma}})$, and τ runs over all the nearest neighbors. These kinds of correlations may be particularly important if several different ordered states compete with each other. In the present case, when the atom density satisfies a specific condition, the superfluid state and the density wave state can be almost degenerate, so that the correlation effects should play a vital role to determine the ground state properties, as will be shown below.

Before proceeding to the discussion on correlation effects, we first examine a spatially modulated superfluid state at the mean-field level. In order to deal with the site-dependent densities and the on-site pairing correlations, we consider the following BdG equations by introducing two kinds of mean-fields $\langle n_{i\sigma}\rangle = \langle c^{\dagger}_{i\sigma} c_{i\sigma}\rangle$ and $\Delta_i = \langle c_{i\downarrow} c_{i\uparrow}\rangle$. The interaction term in the Hamiltonian (1) is then decoupled as $U n_{i\uparrow} n_{i\downarrow} \to U(\langle n_{i\downarrow}\rangle n_{i\uparrow} + \langle n_{i\uparrow}\rangle n_{i\downarrow} + \Delta_i c^{\dagger}_{i\uparrow} c^{\dagger}_{i\downarrow} + \Delta^*_i c_{i\downarrow} c_{i\uparrow} - |\Delta_i|^2 + \text{const})$. In terms of the Bogoliubov transformation $c_{i\sigma} = \sum_\eta \{u^{\eta}_{i\sigma} a_{\eta\sigma} - \sigma v^{\eta}_{i\sigma} a^{\dagger}_{\eta\bar{\sigma}}\}$, we obtain the BdG equations

$$\sum_j \begin{pmatrix} H_{ij\sigma} & F_{ij} \\ F^*_{ji} & -H_{ji\bar{\sigma}} \end{pmatrix} \begin{pmatrix} u^{\eta}_{j\sigma} \\ v^{\eta}_{j\sigma} \end{pmatrix} = E_{\eta\sigma} \begin{pmatrix} u^{\eta}_{i\sigma} \\ v^{\eta}_{i\sigma} \end{pmatrix}, \tag{4}$$

with

$$H_{ij\sigma} = -t\delta_{\langle ij\rangle} + (V_i - \mu + U\langle n_{i\bar{\sigma}}\rangle)\delta_{ij}, \tag{5}$$

$$F_{ij} = U\Delta_i \delta_{ij}, \tag{6}$$

where $a^{\dagger}_{\eta\sigma}$ ($a_{\eta\sigma}$) is the creation (annihilation) operator of a Bogoliubov quasiparticle and $\delta_{\langle ij\rangle}$ is the Kronecker δ for the nearest-neighbor sites between i and j. The corresponding self-consistent equations read

$$\langle n_{i\sigma}\rangle = \sum_\eta |v^{\eta}_{i\sigma}|^2, \tag{7}$$

$$\Delta_i = -\sum_\eta u^{\eta}_i v^{\eta *}_i. \tag{8}$$

Then by means of Pong's method [39], we end up with the following state:

$$|\Phi\rangle = \prod_n (U_n + V_n \gamma^{\dagger}_{n\uparrow} \gamma^{\dagger}_{n\downarrow}) |0\rangle \tag{9}$$

$$\sim \left[\sum_n \frac{V_n}{U_n} \gamma^{\dagger}_{n\uparrow} \gamma^{\dagger}_{n\downarrow} \right]^{N/2} |0\rangle$$

$$= \left[\sum_{ij} \left(\sum_n \frac{V_n}{U_n} \phi^n_i \phi^n_j \right) c^{\dagger}_{i\uparrow} c^{\dagger}_{j\downarrow} \right]^{N/2} |0\rangle, \tag{10}$$

where $|0\rangle$ is the vacuum state and $U_n = \chi_n/\sqrt{|\lambda_n|}$, $V_n = \sqrt{|\lambda_n|}$. $\gamma^{\dagger}_{n\sigma} = \sum_i \phi^n_i c^{\dagger}_{i\sigma}$ is a creation operator of the fermion which contributes to a Cooper pair [39] and is expressed by the linear combination of $c^{\dagger}_{i\sigma}$. χ_n, λ_n are the eigenvalues

of the normal density matrix $\rho_{ij} = \langle c^{\dagger}_{i\sigma} c_{j\sigma} \rangle = \sum_n v^n_i v^{n*}_j$ and the anomalous density matrix $\nu_{ij} = \langle c_{i\downarrow} c_{j\uparrow} \rangle = -\sum_n u^n_i v^{n*}_j$, respectively. $\{\phi^n_i\}(\in \mathbf{R})$ is a set of their simultaneous eigenvectors and called a natural orbit. As the number of atoms in the superfluid state $|\Phi\rangle$ in Eq. (9) is inherently uncertain, we here restrict our analyses in a subspace with fixed atom numbers $N_\uparrow = N_\downarrow = N/2$.

Let us now study the ground-state properties by the VMC simulations [40] to analyze the original Hubbard Hamiltonian Eq. (1). Here we make use of the trial state Eq. (3) with the variational parameters $(\{\alpha_i\}, \alpha', \{\Delta_i\})$. In order to deduce a good trial state with a proper distribution of Δ_i, we take into account a mean-field solution of the BdG Eqs. (4) which is derived from the original Hamiltonian. We wish to note that the interaction U in the BdG equations is not necessarily identical to the bare interaction in the original Hamiltonian, because correlation effects cannot be incorporated sufficiently in the BdG mean-field method. Therefore, we make use of $\{\Delta_i\}$ obtained by the BdG equations with various U in a trial state for given U in the original Hamiltonian [32]. We also note that the VMC method cannot be used for a large (experimental-size) system, in comparison with other variational methods, for example, a recent Gutzwiller variational method for a bosonic atoms in an optical lattice with 560 000 sites [41]. In that study, the trial wave function is described by the site-dependent Gutzwiller factors and the wave function which is written by the product of the local states. On the other hand, in our method, we have introduced two types of Gutzwiller factors, where not only on-site correlations but also intersite correlations are taken into account. Furthermore, we have introduced the wave function obtained from the BdG equations with an additional variational parameter U, which is not the simple product of local states. These enable us to describe the spatially modulated superfluid state more precisely, although it is much more expensive to optimize the trial ground state. Namely, it is known that this treatment with two kinds of Gutzwiller factors and a variational parameter for the wave function is important in discussing ground-state properties of the 2D repulsive Fermionic Hubbard model [42]. In the following calculations, we set $L = 20$, $V_0 = 12$, and $N_\uparrow = N_\downarrow = 80$.

We first show the density profiles $\langle n_i \rangle$ and the pair potentials Δ_i in Figs. 1(a) and 1(b), respectively. When $U < U_c$ (∼2.0), we find that the pair potentials Δ_i are almost zero for all the sites, implying that the ground state is not a superfluid, but a normal metallic state. This is in contrast to the known results for uniform bulk systems, where the superfluid state is always realized for any finite attractive interaction. For $U > U_c$, on the other hand, the pair potentials become finite and the superfluid state is realized. Here we can see that Δ_i are large in the regions with intermediate atom densities; that is, $\langle n_i \rangle \sim 1.0$. For sufficiently large U, a portion of atoms gather around the center of the system, forming a band insulating region with $\langle n_i \rangle \sim 2.0$ and $\Delta_i \sim 0$. We note here that the Gutzwiller correlation factors $\{\alpha_i\}$ play a crucial role in reducing the effective strength of attractive interaction. Actually, we find that the mean-field treatment overestimates the pair potentials substantially; for example, for $U = 4.0$ in Fig. 1(b), we end up with the profile of Δ_i similar to that for $U = 7.0$ if we neglect

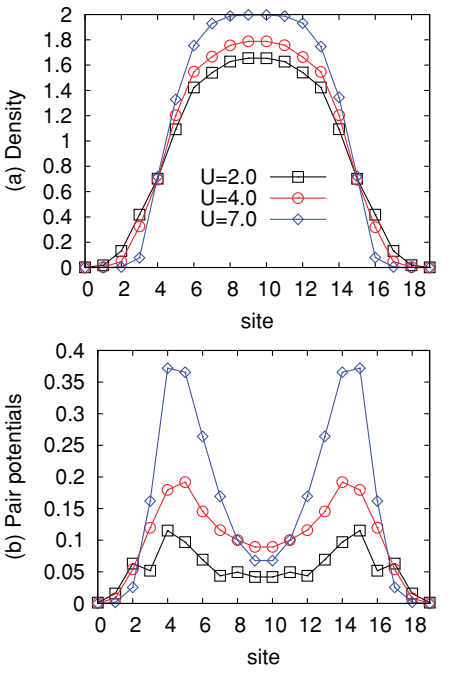

FIG. 1. (Color online) (a) Density profiles $\langle n_i \rangle$ and (b) pair potentials Δ_i along the $y = L/2$ line of the system for $U = 2.0$ (squares), 4.0 (circles), and 7.0 (diamonds). All the data are obtained by the VMC method with sufficiently large samples (∼10^6). Statistical errors are less than the size of the symbol for each point.

$\{\alpha_i\}$. Therefore, we can say that the Gutzwiller correlations, which are usually neglected in the mean-field treatments, are indispensable in discussing the stability of the superfluid state quantitatively.

Next we investigate the intersite density correlation functions to discuss the superfluid properties more precisely. Shown in Fig. 2(a) is the difference of the density correlations between the nearest-neighbor and the next-nearest-neighbor sites, which is defined by $\Delta D_i \equiv \frac{1}{4}\{\sum_\tau \{\langle n_i n_{i+\tau} \rangle - \sum_{\tau'} \langle n_i n_{i+\tau'} \rangle\}$, where τ (τ') runs over all the nearest (next-nearest) neighbors. In a high-density region, this quantity is positive, indicating that the short-range nearest-neighbor density correlations are developed due to the localization of the atoms (band insulating region). It should be noticed here that this quantity becomes negative around $i = 4$

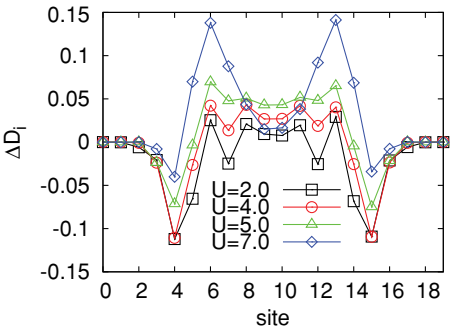

FIG. 2. (Color online) Difference of the density correlations ΔD_i (see text) along the $y = L/2$ line of the system for $U = 2.0$ (squares), 4.0 (circles), 5.0 (triangles), and 7.0 (diamonds).

and 15 sites, implying that the density correlations between the next-nearest-neighbor sites are larger than those between the nearest-neighbor sites. This unusual behavior suggests that the spatially extended correlations with an alternating modulation of density wave with two-site periodicity are enhanced considerably. These results are consistent with those for the homogeneous systems, where the superfluid and the density wave state are degenerate at half-filled band ($\langle n_i \rangle = 1.0$) [43,44]. We can see such a tendency to density wave formation by considering only the Gutzwiller correlations for a trial state in our analysis. As mentioned earlier, the Gutzwiller correlations suppress the superfluidity, and therefore the density wave correlations effectively become enhanced. We also see that the amplitude of ΔD_i is increased for large U in the presence of the intersite spinon-spinon correlations, which suggests that the intersite correlations also support the strong density wave correlations. Here we mention the difference with different dimensionality for the formation of the density wave state. It is well known that in 1D, the Peierls instability has a tendency to induce the density wave state for any particle density. In the present 2D square lattice, however, the density wave can be realized only when the commensurability condition is satisfied for homogeneous systems. In our inhomogeneous case with a trap potential, the density wave could appear in the region where the commensurability condition is approximately satisfied, but it is still subtle whether such a density wave state is stabilized in the presence of superfluidity. This is a nontrivial issue we address in this article.

Finally, we briefly comment on scaling behavior of the region where the density wave correlations are enhanced. As discussed earlier, it is difficult to perform directly finite size scalings due to technical problems in our VMC method. It has, meanwhile, been clarified by means of the real-space dynamical mean-field theory that the profiles of the pair potential and the particle density are well scaled [29]. Therefore, we believe that the region with the enhanced correlations we discuss here should appear even for larger system sizes.

Summarizing the preceding results, we can say that the superfluid state around the regions with $\langle n_i \rangle \sim 1.0$ has a strong tendency to induce a density wave state with checkerboard pattern, which may be enhanced by the correlation effects between atoms. In our VMC analysis, however, we have not found a real instability to such a density wave order in the density profiles and the density structure factor (not shown). Anyway, since such a tendency to form the coexisting state of superfluid and checkerboard density wave, that is, a sort of supersolid state, is enhanced, the system may be immediately driven to the coexisting state once relevant perturbations which stabilize a density wave state are introduced. In the next section, we address this issue.

IV. INSTABILITY TOWARD DENSITY WAVE STATE

In this section, we introduce two kinds of perturbations which may induce a checkerboard-type density wave state and investigate the response by mean-field analyses. First, we consider a staggered potential superposed on the harmonic trap potential, $V_i \to V_i + (-1)^i \Delta V$, which can be experimentally

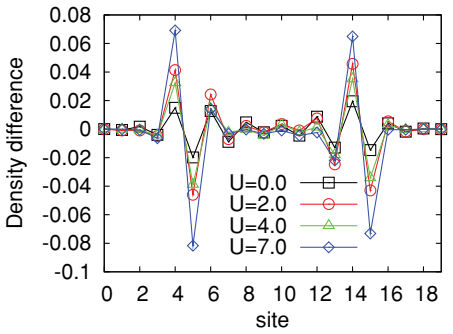

FIG. 3. (Color online) Density difference between the result for $\Delta V = 0$ and 0.02 along the $y = L/2$ line of the system for $U = 0.0$ (squares), 2.0 (circles), 4.0 (triangles), and 7.0 (diamonds).

controlled by superlattice potentials [45]. Here we set $\Delta V = 0.02$, which is much smaller than the potential difference between any adjacent sites. By solving the BdG equations (4) self-consistently, we obtain the density distributions for $\Delta V = 0.02$. Though the obtained density distributions are smooth for small ΔV, we can see a notable difference in the quantity $\langle n_i \rangle_{\Delta V=0.02} - \langle n_i \rangle_{\Delta V=0}$, which is shown in Fig. 3. Around the lattice sites labeled as $i = 4$ and 15, where $\langle n_i \rangle \sim 1.0$, it is seen that a very small perturbation ΔV can give rise to a change in the density profile, and more remarkably it is considerably enhanced as U increases. This reflects the fact that these regions have a tendency toward the formation of the density wave state.

As shown in the previous section, the intersite correlations can support the density wave correlations. Here, we address the effect explicitly by introducing a repulsive interaction $U' \sum_{\langle ij \rangle} n_i n_j (U' > 0)$ between two atoms sitting on nearest-neighbor sites, which might be important for the atoms having dipole-dipole interactions. It is known that the intersite repulsive interactions favor the density wave state under the proper condition mentioned earlier. We here discuss how the density wave states appear in our trapped system. For this purpose, we decouple the additional term as $U' \sum_{\langle ij \rangle} \langle n_i \rangle n_j$, and then add the term $U' \delta_{ij} \{ \sum_k \delta_{\langle ik \rangle} \langle n_k \rangle \}$ to $H_{ij\sigma}$ in Eq. (5). Figure 4(a) shows the density profiles for $U' = 0.02U$. For small interactions, the density distributions seem to be smooth, but we can see that the density wave state indeed appears for $U > 5.0$, mainly around the sites of $i = 4$ and 15, where $\langle n_i \rangle \sim 1.0$ is approximately satisfied for $U' = 0$. This result also reflects the fact that in the region with $\langle n_i \rangle \sim 1.0$ an instability toward the density wave state is enhanced. We have performed similar calculations for $U' = 0.05U$. In this case, it is found that the local densities take the values of $\langle n_i \rangle = 0$ or 2 alternately. Thus, even the small repulsive interaction U' can stabilize the density wave state. In addition, as seen in Fig. 4(b), pair potentials Δ_i have finite values in these regions, which means that the coexisting state of superfluid and density wave is realized there.

All the preceding results demonstrate that the spatially modulated superfluid state at $\Delta V = U' = 0$ has strongly enhanced density fluctuations toward the formation of a checkerboard density wave state in spatial regions satisfying $\langle n_i \rangle \sim 1.0$. Such a tendency, which is enhanced by correlation effects between atoms, is so strong that even tiny perturbations

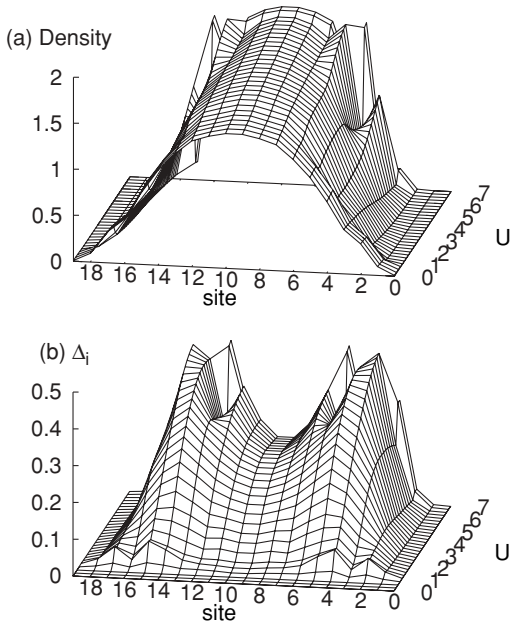

FIG. 4. (a) Density profiles $\langle n_i \rangle$ and (b) pair potentials Δ_i along the $y = L/2$ line of the system obtained with $U' = 0.02U$.

immediately drive the system to a coexisting state with superfluid and density wave ordering. This conclusion seems to be consistent with the claim of Koga *et al.* [29], although we have not found a real instability to the supersolid state at $\Delta V = U' = 0$ within the parameter range studied in this article. There may be a possibility that such a supersolid state can be indeed stabilized even at $\Delta V = U' = 0$ if we consider higher-dimensional systems. This is an interesting problem to be explored in future work.

V. NOISE CORRELATIONS

In order to compare the present results with experiments, it is necessary to consider the experimentally accessible quantities. We therefore discuss in this section how the preceding characteristic features of the superfluid state are reflected in the observable quantities. Here we examine the momentum distributions $\langle n_{\mathbf{Q}\sigma} \rangle$ and the noise correlation functions $G_{\sigma\sigma'}(\mathbf{Q},\mathbf{Q}')$ [46–50], which are evaluated by $|\Phi\rangle$ as

$$\begin{aligned}
\langle n_{\mathbf{Q}\uparrow} \rangle &= \langle c^\dagger_{\mathbf{Q}\uparrow} c_{\mathbf{Q}\uparrow} \rangle \\
&\propto \sum_{ij} e^{i\mathbf{Q}\cdot \mathrm{r}_{ij}} \langle c^\dagger_{i\uparrow} c_{j\uparrow} \rangle \\
&= \sum_{ij} e^{i\mathbf{Q}\cdot \mathrm{r}_{ij}} \sum_{mn} \phi^m_i \phi^n_j \langle \gamma^\dagger_{m\uparrow} \gamma_{n\uparrow} \rangle \\
&= \sum_{ij} e^{i\mathbf{Q}\cdot \mathrm{r}_{ij}} \sum_{n} \phi^n_i \phi^n_j |V_n|^2, \qquad (11)
\end{aligned}$$

$$\begin{aligned}
G_{\sigma\sigma'}(\mathbf{Q},\mathbf{Q}') &= \langle n_{\mathbf{Q}\sigma} n_{\mathbf{Q}'\sigma'} \rangle - \langle n_{\mathbf{Q}\sigma} \rangle \langle n_{\mathbf{Q}'\sigma'} \rangle \\
&= \langle c^\dagger_{\mathbf{Q}\sigma} c^\dagger_{\mathbf{Q}'\sigma'} c_{\mathbf{Q}'\sigma'} c_{\mathbf{Q}\sigma} \rangle \\
&\quad + \delta_{\mathbf{Q},\mathbf{Q}'} \delta_{\sigma,\sigma'} \langle n_{\mathbf{Q}\sigma} \rangle - \langle n_{\mathbf{Q}\sigma} \rangle \langle n_{\mathbf{Q}'\sigma'} \rangle \\
&\propto \sum_{iji'j'} e^{i\mathbf{Q}\cdot \mathrm{r}_{ij} + i\mathbf{Q}'\cdot \mathrm{r}_{i'j'}} \\
&\quad \times \sum_{n_1 \sim n_4} \phi^{n_1}_i \phi^{n_2}_{i'} \phi^{n_3}_{j'} \phi^{n_4}_j \langle \gamma^\dagger_{n_1\sigma} \gamma^\dagger_{n_2\sigma'} \gamma_{n_3\sigma'} \gamma_{n_4\sigma} \rangle \\
&\quad + \delta_{\mathbf{Q},\mathbf{Q}'} \delta_{\sigma,\sigma'} \langle n_{\mathbf{Q}\sigma} \rangle - \langle n_{\mathbf{Q}\sigma} \rangle \langle n_{\mathbf{Q}'\sigma'} \rangle, \qquad (12)
\end{aligned}$$

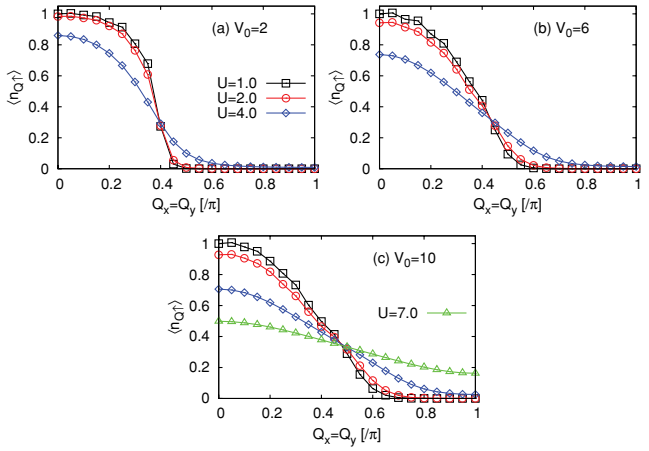

FIG. 5. (Color online) Momentum distributions $\langle n_{\mathbf{Q}\uparrow} \rangle$ ($=\langle n_{\mathbf{Q}\downarrow} \rangle$) for the superfluid state along the line of $\mathbf{Q} = (0,0) \rightarrow (\pi,\pi)$ for $U =$ 1.0 (squares), 2.0 (circles), 4.0 (diamonds), and 7.0 (triangles) ($U' =$ 0). The depth of the trap potential is $V_0 = 2$ (a), 6 (b), and 10 (c). Each $\langle n_{\mathbf{Q}\uparrow} \rangle$ is renormalized by $\langle n_{\mathbf{Q}=\mathbf{0}} \rangle$ for $U = 1.0$.

where $\mathrm{r}_{ij} \equiv \mathbf{r}_i - \mathbf{r}_i$. Note that in Eq. (11) we have used the relation $\langle \gamma^\dagger_{m\sigma} \gamma_{n\sigma'} \rangle = \delta_{\sigma\sigma'} \delta_{mn} |V_n|^2$, which is obtained from Eq. (9). These quantities can be observed by the time-of-flight (TOF) imaging [47]. The momentum $\mathbf{Q}$ and the position $\mathbf{x}$ in the TOF image obtained after ballistic expansion have a relation $\mathbf{Q} = m\mathbf{x}/\hbar t$, where m and t are the mass of atoms and expanding time, respectively. Therefore, the density distributions in the TOF image are expected to reflect the momentum distributions in the trap. In the following calculations, we set $L = 14$ and $N_\uparrow = N_\downarrow = 40$.

We show in Fig. 5 the momentum distributions $\langle n_{\mathbf{Q}\uparrow} \rangle$ ($=\langle n_{\mathbf{Q}\downarrow} \rangle$) for the superfluid state by varying the depth of the trap potential. As seen in Fig. 5(a), $\langle n_{\mathbf{Q}\uparrow} \rangle$ exhibits a characteristic profile similar to the Fermi distribution for a shallow trap and weak interactions, where the ground state is metallic for $U = 1.0$ ($\langle n_i \rangle \sim 1.3$ at the center of the system and $\Delta_i \sim 0$ for all sites) and the superfluid for $U = 2.0$ ($\langle n_i \rangle \sim 1.4$ at the center, and Δ_i have small finite values). As the trap becomes deep, on the other hand, we find that the Fermi distribution is considerably smeared even for small U [(b) and (c)], reflecting the fact that momentum $\mathbf{Q}$ is not a good quantum number anymore. In addition, the increase in the interaction U and the coexisting density wave order [Fig. 5d] further obscures the shape of the momentum distributions. From these computed results, it seems not easy to clarify the characteristic properties of spatially modulated superfluidity experimentally only from the momentum distribution functions.

The noise correlation functions, $G_{\uparrow\downarrow}(\mathbf{Q},-\mathbf{Q})$ between the atoms with momentum $\mathbf{Q}$, spin $\uparrow$ and $-\mathbf{Q}$, $\downarrow$, may be more appropriate to characterize the superfluid state, although the aforementioned smearing effects due to the trap potential emerge even for this quantity, as seen in Fig. 6. Note that the noise correlation functions are directly related to the pair

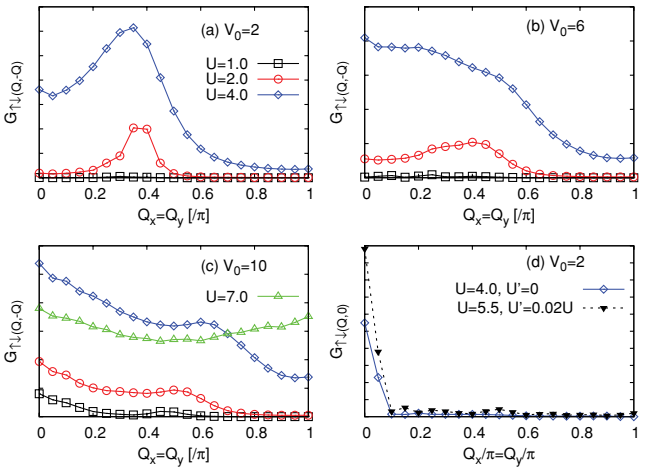

FIG. 6. (Color online) (a–c) Noise correlation functions $G_{\uparrow\downarrow}(\mathbf{Q},-\mathbf{Q})$ along the line of $(0,0) \rightarrow (\pi,\pi)$ for $U = 1.0$ (squares), 2.0 (circles), 4.0 (diamonds), and 7.0 (triangles) ($U' = 0$). The depth of the trap potential is $V_0 = 2$, 6, and 10, respectively. (d) $G_{\uparrow\downarrow}(\mathbf{Q},\mathbf{0})$ for the superfluid state $U = 4.0$, $U' = 0$ (diamonds) and the supersolid state $U = 5.5$ ($U' = 0.02U$) (inverted triangles).

correlations $\langle c_{-\mathbf{Q}\downarrow} c_{\mathbf{Q}\uparrow}\rangle$. We find that a peak structure emerges around the Fermi surface $Q_x = Q_y \sim 0.4\pi$ [see also Fig. 5(a)] for a shallow trap $V_0 = 2$, which clearly signals the formation of superfluidity. It is gradually smeared as the trap potential becomes deep or as the interaction becomes large. For a sufficiently large interaction ($U = 7.0$), as seen in Fig. 6(c), $G_{\uparrow\downarrow}(\mathbf{Q},-\mathbf{Q})$ becomes almost constant for any $\mathbf{Q}$. In this case, there appears a band insulating region around the center of the system and the superfluid state of strongly bound on-site pairs around there. Although we have calculated the momentum distribution function and the noise correlation function for various momenta $\mathbf{Q}$, we have not found any drastic change in 2D contour-plot figures such as the indication of the nodal lines. This originates from the fact that the superfluid state with s-wave-like symmetry is realized in our system. Therefore, we have simply presented the results only along the particular lines in the momentum space.

As shown earlier, the trap potential gives rise to a smearing effect of the noise correlation functions, which is formally analogous to that due to the change in the attractive interaction. For the weak coupling regime like BCS, it may be possible to isolate the smearing effect from the interaction effect, while it may be rather difficult in the strong coupling regime. We think that the smearing effect due to the trap potential may not be negligible even in experimentally accessible systems (~100 sites for each direction), though our analysis here has been restricted to small systems.

We now pose the same questions for the supersolid state. We have calculated the noise correlation functions $G_{\sigma\sigma'}(\mathbf{Q},\mathbf{0})$ in proper conditions for realizing the supersolid state. Note that $G_{\sigma\sigma'}(\mathbf{Q},\mathbf{0})$ reflects both the superfluid correlation $\langle c_{\mathbf{Q}\downarrow} c_{\mathbf{Q}'=\mathbf{0}\uparrow}\rangle$ and the density wave correlation $\langle c^{\dagger}_{\mathbf{Q}\sigma} c_{\mathbf{Q}'=\mathbf{0}\sigma'}\rangle$. Figure 6(d) shows $G_{\uparrow\downarrow}(\mathbf{Q},\mathbf{0})$ for both the superfluid state and the supersolid states. We can find a peak structure around $\mathbf{Q} \sim \mathbf{0}$ in $G_{\uparrow\downarrow}(\mathbf{Q},\mathbf{0})$ for both states, which reflects the fact that the atoms with small momentum $\mathbf{Q} \sim \mathbf{0}$ can contribute to the superfluid state as mentioned earlier. However, we have not found any qualitative differences which characterize the supersolid state, even if a noticeable density wave order coexists with a superfluid order. As suggested for trapped bosonic systems in Ref. [48], there appears just a small peak at $\mathbf{Q} \sim (\pi,\pi)$ for a checkerboard-type density wave state in addition to a strong peak at $\mathbf{Q} \sim \mathbf{0}$ in $G(\mathbf{Q},\mathbf{0})$. The peak is so small that the weak supersolid order is almost indistinguishable from the superfluid order. This is also the case for our fermionic system, so that the corresponding peak structure, which might already be broadened due to the effect of the trap potential in our case, may not be found in our numerical accuracy. This suggests that naive investigations of the noise correlation functions are not sufficient to detect the density wave (supersolid) state. In order to overcome this problem and to detect a signature for the density wave state, alternative methods may be needed. As a possible candidate, we suggest a following recombination method. First, by deepening the lattice potential rapidly, only the density wave order can be kept and the superfluidity is suppressed. Next by controlling the on-site attractive interactions experimentally, two fermions occupying the same site can be transformed into a molecular boson. In this step, each site is occupied by a fermion or a molecular boson. Then the density wave state of bosons may be possibly detected as a peak in the noise correlations.

VI. SUMMARY

We have investigated the 2D Hubbard model with a harmonic trap potential to discuss the superfluid properties of ultracold fermions in an optical lattice. By introducing a trial state with spatially modulated superfluid order parameters, we have performed the VMC calculation to examine how the on-site as well as intersite correlations affect the nature of superfluidity. The analysis has elucidated that the correlation effects give rise to a tendency to the formation of a density wave state with checkerboard pattern locally around the region with $\langle n_i\rangle \sim 1.0$, and indicated that the density wave correlations may be supported by the intersite correlations. Therefore, even a small perturbation of the intersite repulsion U' can stabilize the density wave state coexisting with the superfluid state. We have explicitly confirmed this tendency by considering two kinds of perturbations. As experimentally accessible quantities, we have further discussed how the momentum distributions and the noise correlation functions are affected by the spatial variation of the superfluid state. It has been found in the noise correlation functions that the atoms with even small momenta $\mathbf{Q} \sim \mathbf{0}$, which gradually decrease with increasing interactions, contribute to the superfluid state, the tendency of which becomes much more significant for trapped systems. This quantity may be utilized to analyze the characteristics of the spatially modulated superfluid. On the other hand, the coexisting state (supersolid state) may hardly be detected in the noise correlation patterns. Nevertheless, it may be possibly observed by transforming the fermionic supersolid state into the density wave state of molecular bosons.

In this article, we have restricted our numerical calculations for smaller systems. Although the present analysis suggests that the effect of the trap potential is important to analyze the physical quantities in experiments, more elaborate calculations

for a larger system size close to experimental situations are desirable, which should be done in a future study.

ACKNOWLEDGMENTS

We thank M. Tezuka for valuable discussions. The numerical computations were carried out at the Supercomputer Center, the Institute for Solid State Physics, University of Tokyo. This work is supported by Grant-in-Aids for Scientific Research [Grant Nos. 20740194 (A.K.) and 21540359, 20029013, 20102008 (N.K.)] and the Global COE Program "The Next Generation of Physics, Spun from Universality and Emergence" and "Nanoscience and Quantum Physics" from the Ministry of Education, Culture, Sports, Science, and Technology (MEXT) of Japan. Y.F. is supported by the JSPS. N.K. is supported by Funding Program for World-Leading Innovative R&D on Science and Technology (FIRST Program).

[1] M. Greiner, O. Mandel, T. Esslinger, T. W. Hänsch, and I. Bloch, Nature (London) **415**, 39 (2002).
[2] T. Stöferle, H. Moritz, C. Schori, M. Köhl, and T. Esslinger, Phys. Rev. Lett. **92**, 130403 (2004).
[3] S. Fölling, A. Widera, T. Müller, F. Gerbier, and I. Bloch, Phys. Rev. Lett. **97**, 060403 (2006).
[4] I. Bloch, Nat. Phys. **1**, 23 (2005).
[5] D. Jaksch and P. Zoller, Ann. Phys. **315**, 52 (2005).
[6] O. Morsch and M. Oberthaler, Rev. Mod. Phys. **78**, 179 (2006).
[7] I. Bloch, J. Dalibard, and W. Zwerger, Rev. Mod. Phys. **80**, 885 (2008).
[8] J. K. Chin, D. E. Miller, Y. Liu, C. Stan, W. Setiawan, C. Sanner, K. Xu, and W. Ketterle, Nature (London) **443**, 961 (2006).
[9] A. Koetsier, D. B. M. Dickerscheid, and H. T. C. Stoof, Phys. Rev. A **74**, 033621 (2006).
[10] E. Zhao and A. Paramekanti, Phys. Rev. Lett. **97**, 230404 (2006).
[11] H. Tamaki, Y. Ohashi, and K. Miyake, Phys. Rev. A **77**, 063616 (2008).
[12] G. Orso and G. V. Shlyapnikov, Phys. Rev. Lett. **95**, 260402 (2005).
[13] H. Zhai and T. L. Ho, Phys. Rev. Lett. **99**, 100402 (2007).
[14] E. G. Moon, P. Nikolic, and S. Sachdev, Phys. Rev. Lett. **99**, 230403 (2007).
[15] M. Iskin and C. A. R. Sá de Melo, Phys. Rev. A **78**, 013607 (2008).
[16] C. C. Chien, Y. He, Q. Chen, and K. Levin, Phys. Rev. A **77**, 011601(R) (2008).
[17] A. Moreo and D. J. Scalapino, Phys. Rev. Lett. **98**, 216402 (2007).
[18] M. M. Parish, S. K. Baur, E. J. Mueller, and D. A. Huse, Phys. Rev. Lett. **99**, 250403 (2007).
[19] A. E. Feiguin and F. Heidrich-Meisner, Phys. Rev. B **76**, 220508(R) (2007); Phys. Rev. Lett. **102**, 076403 (2009).
[20] Y. Chen, Z. D. Wang, F. C. Zhang, and C. S. Ting, Phys. Rev. B **79**, 054512 (2009).
[21] M. Iskin and C. J. Williams, Phys. Rev. A **78**, 011603(R) (2008).
[22] M. Rizzi, M. Polini, M. A. Cazalilla, M. R. Bakhtiari, M. P. Tosi, and R. Fazio, Phys. Rev. B **77**, 245105 (2008).
[23] T. K. Koponen, T. Paananen, J.-P. Martikainen, M. R. Bakhtiari, and P. Törmä, New J. Phys. **10**, 045014 (2008).
[24] B. M. Andersen and G. M. Bruun, Phys. Rev. A **76**, 041602(R) (2007).
[25] Y. Fujihara, A. Koga, and N. Kawakami, Phys. Rev. A **79**, 013610 (2009).
[26] F. Karim Pour, M. Rigol, S. Wessel, and A. Muramatsu, Phys. Rev. B **75**, 161104(R) (2007).
[27] G. Xianlong, M. Rizzi, M. Polini, R. Fazio, M. P. Tosi, V. L. Campo Jr., and K. Capelle, Phys. Rev. Lett. **98**, 030404 (2007).
[28] T.-L. Dao, A. Georges, and M. Capone, Phys. Rev. B **76**, 104517 (2007).
[29] A. Koga, T. Higashiyama, K. Inaba, S. Suga, and N. Kawakami, J. Phys. Soc. Jpn. **77**, 073602 (2008); Phys. Rev. A **79**, 013607 (2009).
[30] A. A. Burkov and A. Paramekanti, Phys. Rev. Lett. **100**, 255301 (2008).
[31] H. Yokoyama and H. Shiba, J. Phys. Soc. Jpn. **56**, 1490 (1987).
[32] Y. Fujihara, A. Koga, and N. Kawakami, J. Phys. Soc. Jpn. **76**, 034716 (2007); J. Magn. Magn. Mater. **310**, 882 (2007); Physica B **404**, 3324 (2009).
[33] T. Fukuhara, Y. Takasu, M. Kumakura, and Y. Takahashi, Phys. Rev. Lett. **98**, 030401 (2007).
[34] M. Köhl, H. Moritz, T. Stöferle, K. Günter, and T. Esslinger, Phys. Rev. Lett. **94**, 080403 (2005).
[35] D. Jaksch, C. Bruder, J. I. Cirac, C. W. Gardiner, and P. Zoller, Phys. Rev. Lett. **81**, 3108 (1998).
[36] W. Hofstetter, J. I. Cirac, P. Zoller, E. Demler, and M. D. Lukin, Phys. Rev. Lett. **89**, 220407 (2002).
[37] S. Inouye, M. R. Andrews, J. Stenger, H.-J. Miesner, D. M. Stamper-Kurn, and W. Ketterle, Nature **392**, 151 (1998).
[38] H. Yokoyama, Prog. Theor. Phys. **108**, 59 (2002).
[39] Y. H. Pong and C. K. Law, Phys. Rev. A **74**, 013618 (2006).
[40] S. Sorella, Phys. Rev. B **71**, 241103(R) (2005).
[41] M. Yamashita and M. W. Jack, Phys. Rev. A **76**, 023606 (2007); **79**, 023609 (2009).
[42] T. Watanabe, H. Yokoyama, Y. Tanaka, and J. Inoue, Phys. Rev. B **77**, 214505 (2008).
[43] R. T. Scalettar, E. Y. Loh, J. E. Gubernatis, A. Moreo, S. R. White, D. J. Scalapino, R. L. Sugar, and E. Dagotto, Phys. Rev. Lett. **62**, 1407 (1989).
[44] J. K. Freericks, M. Jarrell, and D. J. Scalapino, Phys. Rev. B **48**, 6302 (1993).
[45] S. Peil, J. V. Porto, B. Laburthe Tolra, J. M. Obrecht, B. E. King, M. Subbotin, S. L. Rolston, and W. D. Phillips, Phys. Rev. A **67**, 051603(R) (2003).
[46] E. Altman, E. Demler, and M. D. Lukin, Phys. Rev. A **70**, 013603 (2004).
[47] T. Rom, Th. Best, D. van Oosten, U. Schneider, S. Fölling, B. Parades, and I. Bloch, Nature (London) **444**, 733 (2006).
[48] V. W. Scarola, E. Demler, and S. Das Sarma, Phys. Rev. A **73**, 051601(R) (2006).
[49] T. Paananen, T. K. Koponen, P. Törmä, and J.-P. Martikainen, Phys. Rev. A **77**, 053602 (2008).
[50] L. Mathey, E. Altman, and A. Vishwanath, Phys. Rev. Lett. **100**, 240401 (2008).